Developmental heatmaps of brain functional connectivity from newborns to 6-year-olds

Haitao Chen [a,b], Janelle Liu [a], Yuanyuan Chen [a], Andrew Salzwedel [a], Emil Cornea [c], John H. Gilmore [c], Wei Gao [a,d,*]

[a] Biomedical Imaging Research Institute (BIRI), Department of Biomedical Sciences and Imaging, Cedars-Sinai Medical Center, Los Angeles, CA, 90048, USA
[b] Department of Bioengineering, University of California at Los Angeles, Los Angeles, CA, 90095, USA
[c] Department of Psychiatry, University of North Carolina Chapel Hill, Chapel Hill, NC, 27599, USA
[d] Department of Medicine, University of California at Los Angeles, Los Angeles, CA, 90095, USA

ARTICLE INFO

ABSTRACT

Different functional networks exhibit distinct longitudinal trajectories throughout development, but the timeline of the dynamics of functional connectivity across the whole brain remains to be elucidated. Here we used resting-state fMRI to investigate the development of voxel-level changes in functional connectivity across the first six years of life. Globally, we found that developmental changes in functional connectivity are nonlinear with more changes during the first postnatal year than the second, followed by most significant changes from ages 2–4 and from ages 4–6. However, the overall global difference observed between the first and second year appears to have been driven by girls. Limbic and subcortical areas consistently demonstrated the most substantial changes, whereas primary sensory areas were the most stable. These patterns were consistent in full-term and preterm subgroups. Validation on randomly divided subsamples as well as in an independent cross-sectional sample revealed global patterns consistent with the main results. Overall, the derived developmental heatmaps reveal novel dynamics underlying functional circuit development during the first 6 years of life.

1. Introduction

The study of early brain functional development through the lens of functional connectivity using resting-state functional magnetic resonance imaging (rsfMRI) has become a burgeoning new field in the past decade (Doria et al., 2010; Fransson et al., 2007; Gao et al., 2009, 2017; Gao et al., 2015a, b; Gilmore et al., 2018; Smyser et al., 2010). The vibrant growth of this field may be partially attributed to the increasing recognition of the developmental origins of various mental disorders and brain diseases (Monk et al., 2019; Wadhwa et al., 2009). Indeed, early identification of risk based on novel imaging techniques, including rsfMRI, has emerged in recent years (Brenner et al., 2020; Gao et al., 2019, 2020; Salzwedel et al., 2019). The NIH's Healthy Brain and Child Development initiative (HBCD; Volkow et al., 2020) precisely recognizes the critical nature of this period and aims to delineate multifaceted brain and behavioral growth during the first 10 years of life with advanced neuroimaging and comprehensive monitoring of potential environmental risks, representing an unprecedented opportunity to shed novel insight into this important developmental period.

Existing studies of early functional connectivity development highlight nonlinear growth trajectories of functional networks critical for early socioemotional development, including default-mode, salience, hippocampus, and amygdala functional networks (Atzil et al., 2018; Gao et al., 2009, 2015a; Salzwedel et al., 2019). The emergence of lateralized functional connectivity among key language network nodes has also been demonstrated during the first two years of life (Fransson et al., 2007; Gao et al., 2009, 2017; Gao et al., 2015a, 2015b; Manning et al., 2013), which is in line with the emergence of initial language function during this period (Conboy et al., 2008). Moreover, thalamocortical functional connectivity has also been shown to experience continuous differentiation and optimization during the same period, and such subcortical-cortical connectivity development indexes later behavioral outcomes (Alcauter et al., 2014). Overall, across the early childhood period, the first two years of life have been more extensively studied (Gao et al., 2017; Gilmore et al., 2018) compared with age three and beyond, which may partly be related to the increasing difficulty of

imaging three- to six-year-olds, either during natural sleep or awake states.

Another prominent gap in our understanding of functional brain development during infancy and early childhood is the lack of a set of whole-brain maps delineating where functional connectivity patterns develop the fastest/slowest across each age span. Much like prior delineations of the structural growth rates of different regions (Gilmore et al., 2018), such maps may reveal "critical regions" at each age span (i. e., those developing the fastest across the age span) or "critical developmental periods" of a given brain region (i.e., the age span during which it develops the fastest). This information regarding the critical regions and/or developmental periods may greatly enrich our understanding of early brain functional development and offer essential guides for targeted prevention and intervention (Gao et al., 2017, 2019). However, previous studies using either a seed-based approach or independent component analysis (ICA; Hyvärinen and Oja, 2000) are not suitable for answering these questions (Lee et al., 2013). Thus, novel approaches need be employed to characterize such functional brain development "heatmaps".

In this study, we propose two steps to bridge the two research gaps. First, we examined functional connectivity development from birth to 6 years of life based on longitudinal rsfMRI scans of a cohort of 655 infants and young children, 266 of whom had at least two successful rsfMRI scans at two consecutive age points (i.e., neonates to 1-year-old (0−1), 1-year-old to 2-year-old (1−2), 2-year-old to 4-year-old (2−4) and 4-year-old to 6-year-old (4−6)). Second, we employed a novel BrainSync method (Joshi et al., 2018) to quantify voxel-wise functional connectivity pattern changes across each of the four age spans (i.e., 0−1, 1−2, 2−4, and 4−6) to create a set of "functional development heatmaps" across the first six years of life. BrainSync was designed to synchronize rsfMRI timeseries across different subjects or across different sessions of the same subject such that similarities/changes in functional connectivity between two subjects/sessions can be quantified by calculating correlations of the synchronized timeseries. This method is used here to synchronize rsfMRI BOLD timeseries of the same subject at two consecutive age points to quantify developmental changes of voxel-wise functional connectivity patterns across each of the four examined age spans. Regions showing the fastest/slowest developmental changes were detected to better inform the "critical regions" across any given age span and "critical developmental periods" for any given region. Sex effects on the derived developmental patterns were specifically examined. We expected to detect nonlinear growth patterns globally and region-specific growth trajectories locally with more changes in higher-order association areas than in primary areas (Gao et al., 2017; Gao et al., 2015a). Based on our large sample size, we conducted three validation analyses to test the robustness of the derived heatmaps. First, we split our sample into a full-term cohort and a moderately preterm cohort (less than 37 weeks gestational age at birth). Given that the preterm infants included in this study were only moderately preterm with a mean gestational age of 34.28 weeks (range 30–36.86 weeks), we expected similar developmental heatmaps between the two cohorts (Cserjesi et al., 2012; Jiang and Wilkinson, 2008). Second, we split our sample into two random cohorts and similar heatmaps were again expected. Lastly, we used an independent cross-sectional sample to test whether the patterns observed in a purely longitudinal sample (i.e., each heatmap was derived based on subjects with data from both age points) could be generalized to cross-sectional samples. To our knowledge, this is the first study to quantify the differential degrees of developmental changes of functional connectivity across different areas of the whole brain during the first six years of life.

2. Material and methods

2.1. Participants

Infant participants were part of the University of North Carolina

Early Brain Development Study, characterizing early childhood brain and behavior development (Gao et al., 2017; Gilmore et al., 2018). Informed consent was obtained from parents/legal guardians of infant participants under protocols approved by the University of North Carolina at Chapel Hill and Cedars-Sinai Institutional Review Board (IRB). After quality control, a cohort of 655 subjects (full-term: N = 364, pre-term: N = 291) with successful rsfMRI scans for at least one time point were retrospectively identified and included in this study. Time points included 3 weeks (neonate), 1 year, 2 year, 4 year, and 6 year. Among them, 266 subjects (full-term: N = 140, preterm: N = 126) had successful rsfMRI scans on at least two consecutive time points. Consecutive time points included 3 weeks and 1 year (0−1), 1 year and 2 year (1−2), 2 year and 4 year (2−4), as well as 4 year and 6 year (4−6). Participant characteristics are listed in Tables 1 and 2, and the distribution of data is shown in Figure S1. Criteria for determining full-term and preterm required gestational age at birth $> = 37$ weeks or <37 weeks, respectively. Exclusionary criteria included any neonatal illness requiring more than a 24 -h stay at a neonatal intensive care unit, abnormal MRI, major medical/neurologic illness, psychiatric problems, and maternal psychiatric disorder diagnosis.

2.2. Imaging acquisition

Longitudinal rsfMRI data were collected at 3 weeks (neonates), 1 year, 2 years, 4 years, and 6 years of age. All neonate, 1-, and 2-year-old subjects were in a natural sleep state, while all 4- and 6-year-old subjects were awake during the imaging session; all 4-year-olds watched cartoons and 6-year-olds watched either cartoons (different cartoons at each time point) or a fixation cross. Additional analyses were conducted to ensure that brain state did not affect the results (discussed below). All MRI data were collected on a Siemens 3 T Allegra (circular polarization head coil) or Tim Trio scanner (32-channel head coil). Functional images were acquired using a T2*-weighted echo planar imaging (EPI) sequence: TR = 2000 ms, TE = 32 ms, 33 slices, voxel size = 4mm^3, 150 volumes. Structural images were acquired using a three-dimensional magnetization prepared rapid acquisition gradient-echo (MPRAGE) sequence: TR = 1820 ms, TE = 4.38 ms, inversion time = 1100 ms, voxel size = 1mm^3.

2.3. fMRI data preprocessing

Functional imaging data were preprocessed using FMRIB's Software Library (FSL; Smith et al., 2004) and Analysis of Functional Neuroimages (AFNI; Cox, 1996). Preprocessing included discarding the first three volumes, rigid-body motion correction, bandpass filtering (0.01–0.08 Hz), and nuisance signal regression. The nuisance signal regression model included 32-parameters (32 P); eight regressors corresponded to white matter (WM) and cerebral spinal fluid (CSF) signals and the remaining parameters included six motion estimates as well as their derivative, quadratic, and squared derivative terms (Power et al., 2014). All nuisance signals were band-pass filtered (0.01–0.08 Hz)

Table 1
Subject demographics for all subjects with data for at least one time point.

Subjects (N = 655; 344 Male)	Mean (SEM)
Gestational Age at Birth (Weeks)	36.90 (0.11)
Birth Weight (Grams)	2721.82 (27.03)
Maternal Age at Birth (Years)	30.13 (0.23)
Maternal Education (Years)	15.20 (0.13)

Age Group	N
Neonate	444
One-year	299
Two-year	228
Four-year	128
Six-year	151

Table 2

Subject demographics for subjects with data for at least two consecutive time points.

Subjects (N = 266; 141 Male)	Mean (SEM)
Gestational Age at Birth (Weeks)	36.74 (0.18)
Birth Weight (Grams)	2701.98 (42.74)
Maternal Age at Birth (Years)	29.79 (0.36)
Maternal Education (Years)	15.20 (0.20)
Age Span	N
0−1	189
1−2	133
2−4	56
4−6	50

before regression to match the frequency of the blood oxygenation level dependent (BOLD) signal. Data scrubbing (Power et al., 2012) was performed as an additional motion correction step in addition to the standard rigid-body motion correction procedures. Volumes with frame-wise displacement (FD) > 0.3 mm were removed (i.e., "scrubbed") from the data; if fewer than three volumes remained between the scrubbed volumes, then these volumes were also removed (Power et al., 2012). Subjects with fewer than 90 volumes remaining after scrubbing were excluded from the study. Global signal regression was performed to regress out the mean grey matter signal from the data. The data were spatially smoothed with a Gaussian kernel of 6 mm full width at half maximum (FWHM) and truncated to 90 volumes. Spatial registration to an infant brain template (Shi et al., 2011) was performed using a two-step approach: 1) subject-specific linear functional-to-anatomical (FLIRT, a fully automated robust and accurate tool for linear intra- and inter-modal brain image registration, i.e., it will translate, rotate, zoom, and shear one image to match with another; Jenkinson et al., 2002) plus age-specific nonlinear anatomical-to-standard warping (FNIRT, a tool for small-displacement nonlinear registration where the displacement fields are modelled as linear combinations of basis-functions and registration is based on a weighted sum of scaled sum-of-squared differences and membrane energy; Andersson et al., 2007), and 2) between-age-group linear transformations (FLIRT; Jenkinson et al., 2002). The 2-year template (Shi et al., 2011) served as the final target for spatial registration; rsfMRI data across all ages were aligned to the same 2-year template space for subsequent BrainSync analyses.

2.4. fMRI data analysis

2.4.1. BrainSync analysis

BrainSync (Joshi et al., 2018) is a novel method capable of synchronizing rsfMRI timeseries across subjects or sessions such that similarities in functional connectivity between two subjects or sessions can be quantified by calculating correlations of the synchronized timeseries. An orthogonal transformation is used to synchronize rsfMRI timeseries such that higher correlation values reflect greater similarity between connectivity patterns at the same voxel across subjects and sessions. Thus, voxel-wise correlations of synchronized timeseries between different subjects and sessions indicate the similarity of their functional connectivity patterns. For the present study, BrainSync was used to synchronize the timeseries across two different age points for each subject. Then, voxel-wise correlation values were calculated based on the synchronized timeseries between the two age points to form a whole-brain heatmap quantifying developmental changes of functional connectivity at each voxel (i.e., one minus correlation was calculated at each voxel to indicate the degree of difference between the two time points). Average heatmaps across all subjects for each age span (0−1, 1−2, 2−4, and 4−6) were calculated to characterize age-span-specific developmental heatmaps. In order to statistically quantify the developmental changes, the change values (i.e., one minus correlation) were Fisher-*Z* transformed to meet statistical assumptions. The whole-brain-level change value for each subject was calculated as the average change value across all voxels within the whole-brain mask. Next, a group-level average whole-brain-level change value across all subjects was calculated for each age span to characterize age-span-specific whole-brain-level developmental changes.

Voxel-wise two-sample *t*-tests (AFNI's 3dttest++, which performs Student's *t*-test of sets of 3D datasets; Cox, 1996) were used to further quantify between-group (e.g., full-term versus preterm) differences. Significance was defined using a clustering approach (AFNI's 3dClustSim, which computes a cluster-size threshold for a given voxel-wise *p*-value threshold by simulating noise volume assuming the spatial auto-correlation function is given by a mixed-model, such that the probability of anything surviving the dual thresholds is at some given level) to achieve the desired correction rate of $\alpha = .05$. Specifically, a voxel-wise cutoff of $p < .001$ was imposed and smoothness estimates from the preprocessed data were generated using the mixed-model autocorrelation function. Minimum cluster sizes (bi-sided, nearest neighbor=1) were then established using AFNI's 3dClustSim. Whole-brain-level mean changes across voxels within the whole-brain mask were obtained for each subject, and significant differences ($p < .05$) between different age spans were established using *t*-test and FDR correction (Benjamini and Hochberg, 1995).

2.4.2. Network-level analysis

To further examine developmental changes at the network level, a seven-network parcellation (visual, somatomotor, dorsal attention, ventral attention, limbic, frontoparietal, default mode network; Yeo et al., 2011) as well as a subcortical network (consisting of the remaining cortical regions including hippocampus, parahippocampal gyrus, amygdala, caudate, putamen, pallidum, and thalamus) were applied and the mean changes across voxels within each network were calculated for each age span. Specifically, each network mask was first registered to 2-year template space using FSL's FLIRT (Jenkinson et al., 2002). Next, mean changes across voxels within each network were obtained for each age span by masking the developmental change maps by each network mask. The average mean changes within each network were subsequently ranked in descending order within each age span.

2.4.3. Critical regions analysis

An automated anatomical labeling (AAL) parcellation in 2-year space (Shi et al., 2011) was used to divide the brain into 90 regions of interest (ROIs). ROI-specific developmental change values were calculated as the average change across voxels within each ROI for each subject's heatmap. A one-sample two-sided *t*-test was performed on ROI-specific changes across different subjects against the whole-brain-level mean change for each age span. Significant ($p < .001$, FDR-corrected) ROIs were selected and ranked based on mean change value across subjects. Critical regions (i.e., significant top- or bottom-ranking ROIs) were further identified and common critical ROIs that consistently showed significantly greatest or fewest changes across all four age spans were also characterized.

2.4.4. Seed-based functional connectivity analysis

To provide illustrative examples of the longitudinal development of functional connectivity, a seed-based functional connectivity analysis was conducted using the common critical ROIs (i.e., top- or bottom-ranking ROIs in the age-span-specific heatmap). For each common critical ROI, a seed region was defined as an 8mm-radius sphere around the peak of the ROI. The average fMRI time series within the seed region was extracted and correlated with every other voxel in the brain to form a seed-based functional connectivity map for each subject in each age group. After Fisher-*Z* transformation, voxel-wise one-sample *t*-tests (AFNI's 3dttest++; Cox, 1996) were used to quantify the age-group-level functional connectivity maps. Significance was defined using a clustering approach (AFNI's 3dClustSim) to achieve the desired correction rate of $\alpha = .05$. A voxel-wise cutoff of $t>3.3339$ ($p\sim.001$) was

imposed on all five age groups for consistency. The age-group-level functional connectivity maps based on top-ranking regions were also obtained in boys and girls separately, following the same steps. Next, mean functional connectivity matrices (Power et al., 2011) organized by networks were obtained for each age group. Specifically, the average time series for each of 90 ROIs was extracted based on the AAL template (Shi et al., 2011) and a 90-by-90 functional connectivity (Fisher-Z transformed) matrix was calculated for each individual subject. Subject-level functional connectivity matrices were then averaged to generate a mean functional connectivity matrix for each age group.

2.5. Testing different demographic variables and validation

We conducted four additional analyses to 1) determine sex effects in our sample, 2) assess whether term status influenced the results, 3) test replicability of the results by randomly splitting the sample into subgroups, and 4) validate the results in an independent sample of subjects with solely cross-sectional data. To determine sex effects within our sample, males (N = 141) and females (N = 125) were identified from the original cohort (N = 266; subjects with data on at least two consecutive time points) (Table S1). To assess whether term status influenced the results, the original cohort was divided based on full-term (N = 140) and preterm (N = 126) status (Table S2). To test replicability of the main findings, we conducted three random splits, where each random split yielded two random subgroups balanced by sex distribution (Table S3). The same analytical steps (as described above) were applied to each subgroup to generate the age-span-specific developmental heatmaps and whole-brain-level developmental changes. Lastly, a pairwise method was applied to a cross-sectional sample (i.e., subjects with data only at separate time points; N = 389; Table S4). Specifically, the same steps were replicated on subject pairs from one age group to another (instead of on the same subjects), then the average heatmaps across all subject pairs for each age span (i.e., 0−1, 1−2, 2−4, 4−6) were calculated to form the age-span-specific developmental heatmaps and whole-brain-level developmental changes. Voxel-wise two-sample t-tests (AFNI's 3dttest++; Cox, 1996) were used to further quantify between-group differences. For all replication and validation analyses, voxel-level significance was defined using a clustering approach (AFNI's 3dClustSim) to achieve the desired correction rate of $\alpha = .05$ and a voxel-wise cutoff of $p < .001$, and whole-brain-level significance was defined using two-sample t-test and FDR correction (Benjamini and Hochberg, 1995) to achieve the correction rate of $p < .05$.

2.6. Effects of differences in awake brain state

In order to investigate the effects of differences in awake brain state in the 6-year-olds (i.e., watching cartoons or fixation cross), a two-sample t-test was performed on the 4−6 developmental heatmaps. Subjects were separated into subgroups based on 6-year brain status (N = 28 watching cartoons, N = 22 watching fixation cross); since all 4-year-old subjects watched cartoons, these two subgroups either had "similar" brain states (Cartoon-Cartoon; i.e., watched cartoons at 4-year and 6-year scan) or changed in brain state (Cartoon-Cross; i.e., watched cartoons at 4-year scan and fixation cross at 6-year scan) (Table S5). Significance was defined using voxel-level $p = .001$, with cluster correction rate $\alpha = .05$. The 4−6 developmental heatmaps for these brain state subgroups (Cartoon-Cartoon, Cartoon-Cross) were also obtained following the same analytical steps described above.

3. Results

3.1. Longitudinal heatmaps of global developmental changes

Global heatmaps delineating developmental changes in the functional connectivity patterns across different age spans (i.e., 0−1, 1−2, 2−4, 4−6) were obtained using BrainSync synchronization (Fig. 1a). Globally, more overall developmental changes in functional connectivity were observed during the first year (0−1) compared with the second year (1−2) of life ($p = .006$, FDR-corrected; Fig. 1b). However, more changes were observed in 2−4 compared with either 0−1 ($p < .001$, FDR-corrected) or 1−2 ($p < .001$, FDR-corrected), with similar changes observed in 4−6 such that there was no significant difference between 2−4 and 4−6 ($p = .858$, FDR-corrected), but 4−6 showed more changes than either 0−1 ($p = .002$, FDR-corrected) or 1−2 ($p < .001$, FDR-corrected; Fig. 1b).

Spatially, during the first two years of life, developmental changes were observed mostly in limbic areas, whereas 2−4 and 4−6 exhibited widespread developmental changes across the whole brain including limbic and subcortical areas (Fig. 1a). At the network level, limbic and subcortical networks consistently demonstrated the most change across all four age spans, followed by other higher-order networks (including frontoparietal, ventral attention, dorsal attention, default mode),
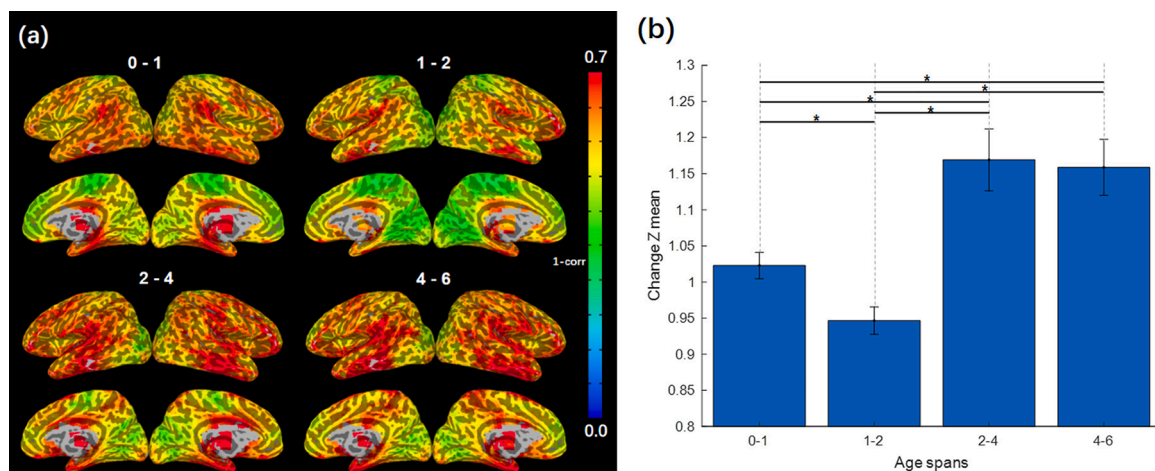

Fig. 1. Developmental changes of functional connectivity across the first six years of life. (a) Global heatmaps of developmental changes show greater changes in limbic areas during the first two years of life, with widespread developmental changes observed for 2-4 and 4-6. Warmer colors (red and yellow regions) indicate more changes whereas cooler colors (blue and green regions) indicate fewer changes. (b) Whole-brain-level developmental changes reveal a nonlinear pattern with more changes occurring during the first (0-1) versus second (1-2) postnatal year, with a spike in changes in 2-4 maintained through 4-6. Mean voxel-wise developmental changes (Fisher-Z transformed) are plotted with standard error of the mean. Significant differences between age spans were tested using t-test (*$p < .05$, FDR-corrected) (For interpretation of the references to colour in the Figure, the reader is referred to the web version of this article).

whereas sensorimotor and visual networks showed the fewest changes over time (Fig. 2).

3.2. Critical regions and examples of seed-based functional connectivity maps

Critical regions showing the largest or smallest developmental changes compared with the group mean ($p < .001$, FDR-corrected) for each age span were identified (Fig. 3, Table 3). Consistent with network level patterns, across all four age spans, common critical regions that consistently showed the most changes were in subcortical and limbic areas, including right thalamus, left parahippocampal gyrus, left inferior temporal gyrus, and right superior frontal gyrus (orbital). In contrast, common regions that consistently showed the fewest changes were more localized to primary visual areas including left cuneus, left superior occipital gyrus, left calcarine cortex, and left paracentral lobule. Examples of seed-based functional connectivity maps for ROIs demonstrating the greatest (i.e., top-ranking; Fig. 4a) and fewest (i.e., bottom-ranking; Fig. 4b) developmental changes were generated. Indeed, functional connectivity maps of "critical" (i.e., top-ranking) regions showed substantial and dynamic changes across all five age points examined (Fig. 4a), whereas those of "bottom" (i.e., bottom-ranking) regions showed similar functional connectivity patterns across all age points (Fig. 4b). Mean functional connectivity matrices organized by networks were also generated (Figure S9). Primary networks (including visual and somatomotor networks) showed fewer intra- and inter-network (e.g., between visual and somatomotor networks) developmental changes while the higher-order networks (including subcortical, limbic and frontoparietal networks) demonstrated more intra- and inter-network (e.g., between subcortical and limbic networks) developmental changes.
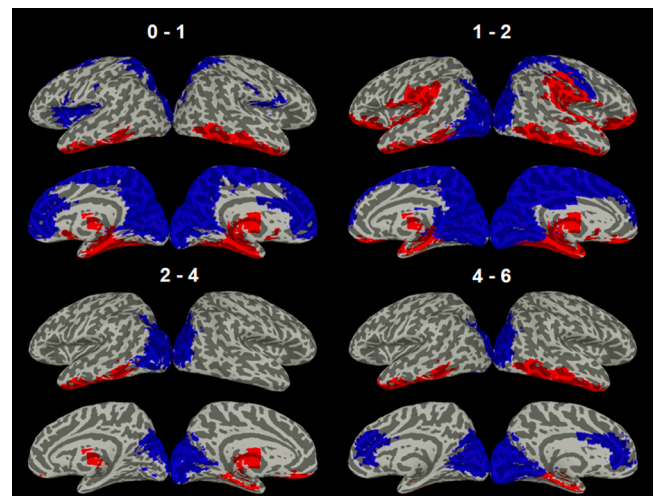

Fig. 3. Critical regions showing significant top- or bottom-ranking developmental changes. Top-ranking regions (in red) showing the most changes over time were in subcortical and limbic areas whereas bottom-ranking regions (in blue) showing the fewest changes over time were mostly localized to primary visual areas (across all age spans) and medial frontal and parietal regions (0-1 and 1-2). (For interpretation of the references to colour in the Figure, the reader is referred to the web version of this article).

3.3. Sex-related differences

In order to examine sex-related effects in our sample, we separated the original cohort into male and female subgroups (Fig. 5). No significant voxel-wise differences were observed between males and females (Fig. 5a). However, females showed more whole-brain-level developmental changes during 0−1 and less change during 1−2 (Fig. 5b; $p < .001$, FDR-corrected) while males showed highly comparable
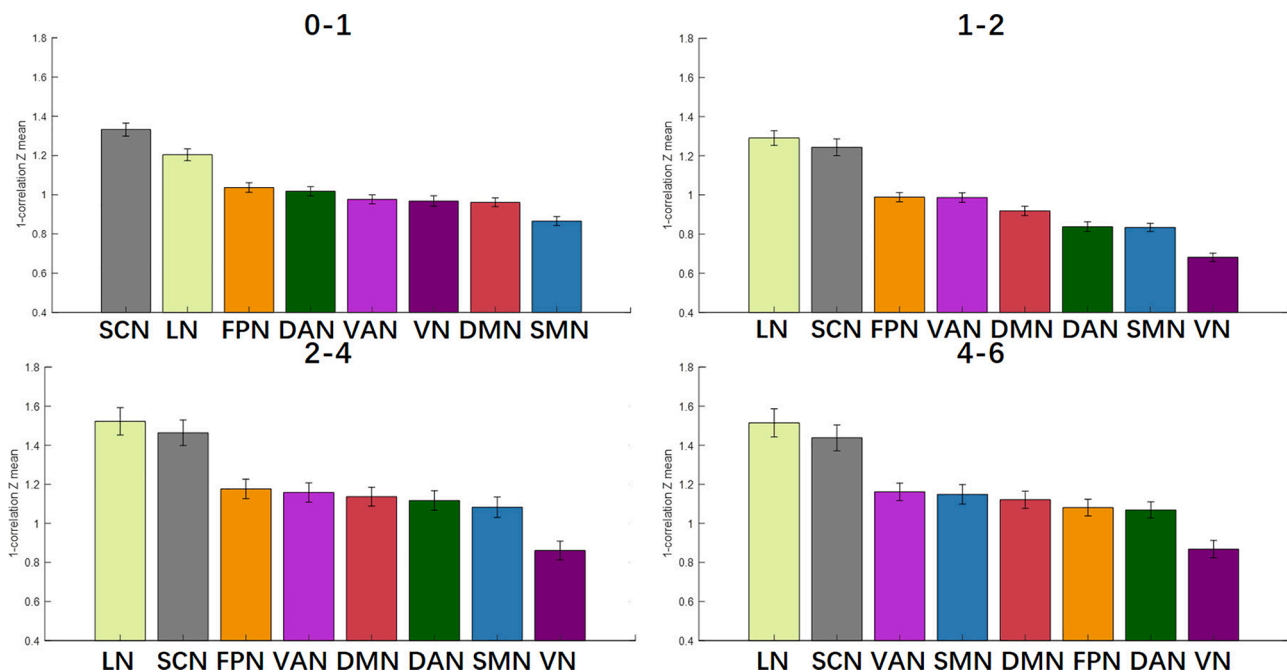

Fig. 2. Network-level developmental changes across the first six years of life. Across all age spans, limbic and subcortical networks consistently show the most change, followed by higher-order networks, with primary sensory networks showing the least change over time. Ranked means are shown for the eight networks examined: visual network (VN; dark purple), somatomotor network (SMN; blue), dorsal attention network (DAN; dark green), ventral attention network (VAN; light purple), limbic network (LN; light green), frontoparietal network (FPN; orange), default mode network (DMN; red), and subcortical network (SCN; gray). Larger values indicate greater changes observed; mean values are plotted with standard error of the mean. (For interpretation of the references to colour in the Figure, the reader is referred to the web version of this article).

Table 3

Critical regions showing significant top- or bottom-ranking developmental changes for each age span.

Top-Ranking Regions[1]	t values[2]	p-values[3]	Bottom-Ranking Regions[1]	t values[2]	p-values[3]
Age Span 0-1					
Thalamus_R	8.821	<.001	Frontal_Sup_L	−4.658	<.001
Thalamus_L	7.600	<.001	Parietal_Sup_R	−4.043	<.001
Hippocampus_R	7.374	<.001	Occipital_Sup_L	−3.757	<.001
ParaHippocampal_L	7.791	<.001	Insula_L	−4.617	<.001
Hippocampus_L	7.487	<.001	Parietal_Sup_L	−4.103	<.001
ParaHippocampal_R	5.97	<.001	Rolandic_Oper_R	−3.777	<.001
Temporal_Inf_R	6.396	<.001	Rolandic_Oper_L	−4.309	<.001
Temporal_Inf_L	5.894	<.001	Occipital_Sup_R	−5.227	<.001
Fusiform_R	5.914	<.001	Frontal_Mid_Orb_L	−4.056	<.001
Caudate_R	4.068	<.001	Calcarine_L	−5.308	<.001
Fusiform_L	5.698	<.001	Calcarine_R	−5.057	<.001
Frontal_Sup_Orb_R	4.120	<.001	Precuneus_R	−6.865	<.001
Caudate_L	4.127	<.001	Precuneus_L	−6.629	<.001
			Cuneus_R	−5.727	<.001
			Cuneus_L	−6.794	<.001
			Frontal_Mid_Orb_R	−5.898	<.001
			Supp_Motor_Area_L	−5.659	<.001
			Frontal_Sup_Medial_R	−6.903	<.001
			Supp_Motor_Area_R	−7.474	<.001
			Cingulum_Ant_L	−7.552	<.001
			Frontal_Sup_Medial_L	−9.481	<.001
			Cingulum_Ant_R	−9.131	<.001
			Paracentral_Lobule_R	−14.473	<.001
			Paracentral_Lobule_L	−19.926	<.001
Age Span 1-2					
Frontal_Sup_Orb_R	7.863	<.001	Postcentral_R	−4.086	<.001
Rectus_R	7.085	<.001	Cingulum_Mid_L	−3.935	<.001
Heschl_L	5.359	<.001	Frontal_Sup_Medial_R	−4.965	<.001
Thalamus_R	5.182	<.001	Parietal_Sup_R	−5.179	<.001
Hippocampus_L	6.878	<.001	Cingulum_Post_R	−3.627	<.001
ParaHippocampal_L	7.531	<.001	Occipital_Inf_L	−3.930	<.001
Thalamus_L	4.460	<.001	Occipital_Mid_R	−5.949	<.001
Frontal_Sup_Orb_L	5.776	<.001	Occipital_Mid_L	−6.786	<.001
Hippocampus_R	6.650	<.001	Frontal_Sup_Medial_L	−5.375	<.001
Temporal_Sup_L	6.743	<.001	Occipital_Sup_R	−6.866	<.001
Frontal_Mid_Orb_R	5.377	<.001	Supp_Motor_Area_L	−7.446	<.001
Temporal_Inf_L	6.827	<.001	Lingual_R	−10.883	<.001
Frontal_Inf_Orb_R	6.725	<.001	Supp_Motor_Area_R	−10.686	<.001
Pallidum_L	3.750	<.001	Lingual_L	−9.988	<.001
Rectus_L	5.099	<.001	Occipital_Sup_L	−10.114	<.001
Frontal_Inf_Orb_L	5.567	<.001	Precuneus_L	−12.132	<.001
SupraMarginal_L	5.377	<.001	Precuneus_R	−11.890	<.001
Temporal_Pole_Sup_L	5.625	<.001	Calcarine_R	−10.706	<.001
Temporal_Inf_R	6.097	<.001	Cuneus_R	−9.259	<.001
Heschl_R	3.634	<.001	Calcarine_L	−12.579	<.001
Frontal_Mid_Orb_L	4.017	<.001	Cuneus_L	−11.836	<.001
Temporal_Sup_R	5.180	<.001	Paracentral_Lobule_R	−18.299	<.001
SupraMarginal_R	4.272	<.001			
Caudate_L	4.033	<.001			
Temporal_Pole_Sup_R	3.698	<.001	Paracentral_Lobule_L	−17.877	<.001
ParaHippocampal_R	4.169	<.001			
Fusiform_L	3.756	<.001			
Age Span 2-4					
Thalamus_R	4.425	<.001	Occipital_Mid_L	−4.968	<.001
Thalamus_L	4.678	<.001	Occipital_Mid_R	−4.701	<.001
ParaHippocampal_L	4.892	<.001	Calcarine_L	−4.466	<.001
Frontal_Sup_Orb_R	5.237	<.001	Occipital_Sup_R	−6.504	<.001
Frontal_Sup_Orb_L	4.780	<.001	Occipital_Sup_L	−5.737	<.001
Rectus_L	4.208	<.001	Cuneus_R	−6.547	<.001
Temporal_Inf_L	4.207	<.001	Cuneus_L	−7.655	<.001
Age Span 4-6					
ParaHippocampal_L	5.214	<.001	Lingual_L	−4.986	<.001
Temporal_Pole_Mid_L	4.192	<.001	Occipital_Mid_R	−5.443	<.001
Temporal_Inf_L	5.371	<.001	Calcarine_L	−5.876	<.001
			Cingulum_Ant_R	−5.699	<.001
			Calcarine_R	−4.623	<.001
			Cingulum_Ant_L	−6.093	<.001
Temporal_Inf_R	4.706	<.001	Occipital_Sup_L	−4.935	<.001
			Cuneus_R	−4.945	<.001
			Occipital_Sup_R	−6.914	<.001
			Cuneus_L	−4.977	<.001

[1] The naming of AAL regions is adopted from Liu et al., 2014.
[2] The *t* values indicate difference between region and whole-brain mean.
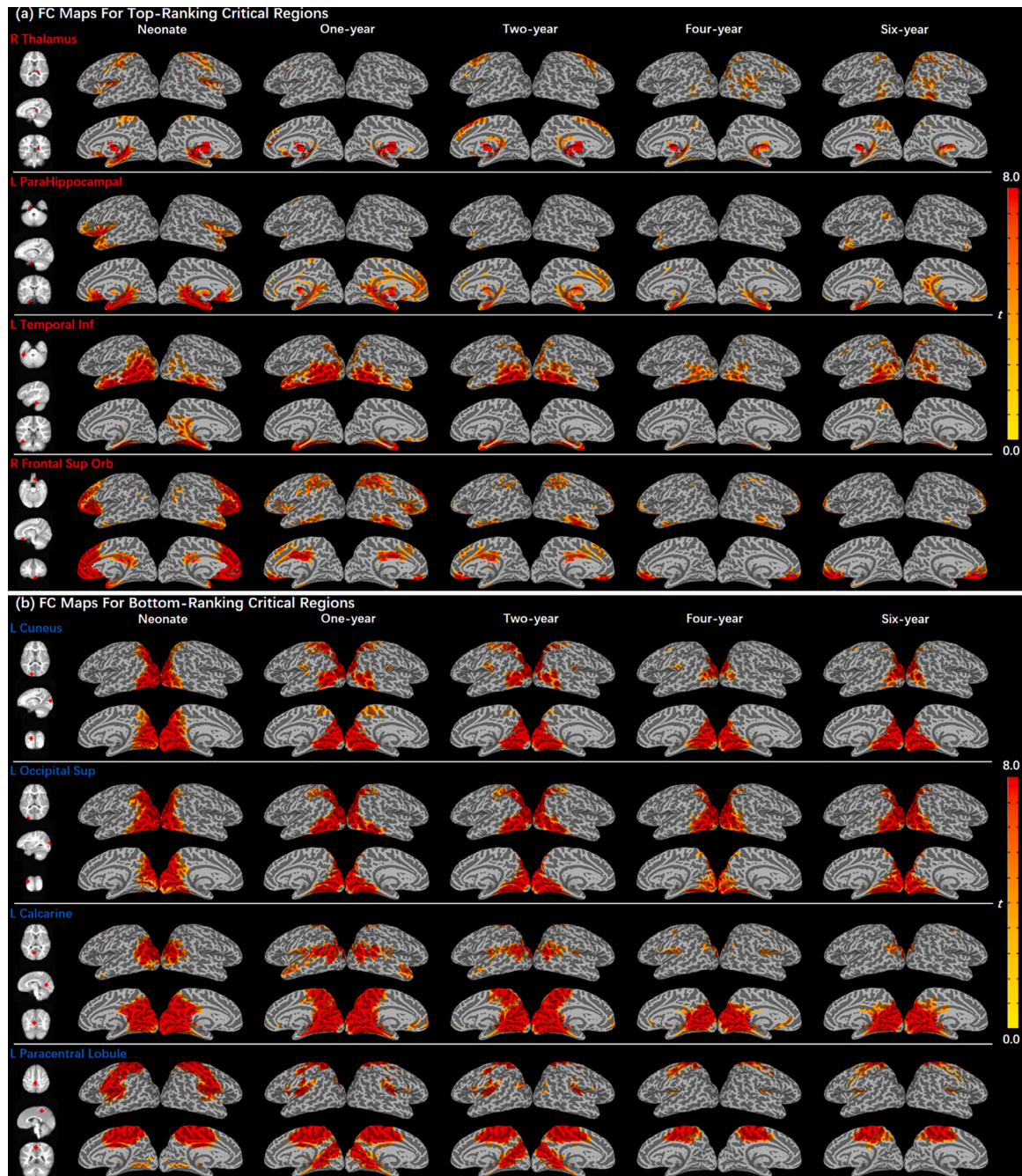[3] The *p*-values are FDR corrected.

Fig. 4. Illustrative examples of developmental trajectories of functional connectivity for top- and bottom-ranking critical regions. (a) Functional connectivity maps for top-ranking regions (including right thalamus, left parahippocampal gyrus, left inferior temporal gyrus, and right superior frontal gyrus) showed dynamic changes over time. (b) Functional connectivity maps for bottom-ranking regions (including left cuneus, left superior occipital sulcus, left calcarine, left paracentral lobule) were stable across time.

changes between the two age spans, suggesting that the global differences we observed in the original cohort with more developmental changes observed during 0−1 compared with 1−2 may have been largely driven by the females in the sample. Seed-based functional connectivity maps of the top-ranking critical regions shown in Fig. 4 confirmed similar patterns (Figure S2). Other global and local patterns were highly consistent across males and females.

3.4. Effects of term status

To assess whether term status could have affected our results, developmental heatmaps across all four age spans and whole-brain-level developmental changes were generated for full-term and preterm subgroups (Figure S3). No significant voxel-wise differences were observed between full-term and preterm infants (Figure S3a). Moreover, both subgroups showed similar patterns in the whole-brain-level
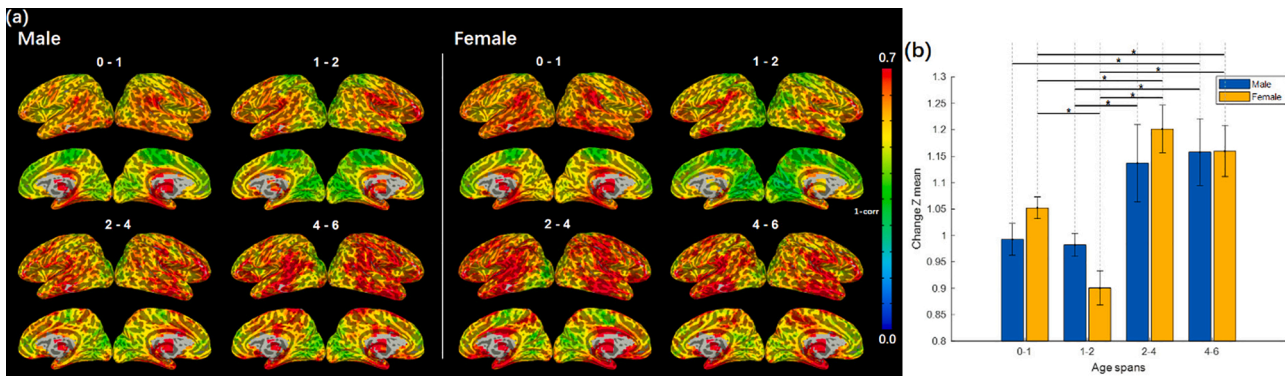
Fig. 5. Developmental changes of functional connectivity across the first six years of life in male and female subgroups. (a) No significant differences were observed between male and female infants in the global heatmaps of developmental changes. Warmer colors (red and yellow regions) indicate more changes whereas cooler colors (blue and green regions) indicate fewer changes. (b) Females showed greater whole-brain-level developmental changes during the first year (0-1) and less change during the second year (1-2) ($p < .001$, FDR-corrected) while males did not show significant differences across the first two years. Other global patterns were similar across males and females, consistent with the whole group patterns shown in Fig. 1. Mean voxel-wise developmental changes (Fisher-Z transformed) plotted with standard error of the mean. Significant differences between age spans were tested using t-test (*$p < .05$, FDR-corrected). (For interpretation of the references to colour in the Figure, the reader is referred to the web version of this article).

developmental changes with more changes observed during 0−1 compared with 1−2 (full-term: $p = .036$, preterm: $p = .087$, FDR-corrected), followed by more changes observed in 2−4 and 4−6 (Figure S3b), paralleling the results observed in the original cohort containing both full-term and preterm infants.

3.5. Replication using random split

To test the robustness of our main findings, we conducted three replication analyses by randomly splitting the sample. Each random split resulted in two random subgroups that were matched on the distribution of males and females to control for sex effects (Table S3, Figures S4, S5, S6). No significant voxel-wise differences were observed between the subgroups for each random split (Figures S4a, S5a, S6a). Whole-brain-level developmental changes observed in each random split were similar to our main finding with more changes occurring during 0−1 than 1−2 (Split 1: Random 1 $p = .041$, Random 2 $p = .100$; Split 2: Random 3 $p = .010$, Random 4 $p = .313$; Split 3: Random 5 $p = .027$, Random 6 $p = .130$; All p-values were FDR-corrected), followed by the greatest changes observed in 2−4 and 4−6 (Figures S4b, S5b, S6b).

3.6. Validation in a cross-sectional sample

Lastly, pairwise developmental heatmaps across all four age spans were generated in a cross-sectional sample (Figure S7). Following cluster correction, fewer than 1% of all voxels showed significant differences between this cross-sectional sample and the original longitudinal cohort (Figure S7a). However, it is important to note that differences between the age spans are more pronounced in this cross-sectional sample since changes between age spans included between-subject differences. Whole-brain-level developmental changes showed similar patterns in the cross-sectional sample compared with the main results (Figure S7b).

3.7. Effects of differences in brain state from 4−6

Effects of changes in brain state were examined in a post-hoc analysis whereby the 4−6 age span was separated into Cartoon-Cartoon (i.e., "similar" brain state from 4−6; watched cartoons at 4-year and 6-year scan) and Cartoon-Cross (i.e., different brain state from 4−6; watched cartoons at 4-year scan and fixation cross at 6-year scan) subgroups (Figure S8). There were no significant voxel-wise differences between these subgroups after cluster correction (Figure S8a). However, the Cartoon-Cartoon subgroup showed more changes than Cartoon-Cross

subgroup at the whole-brain level (Figure S8b).

4. Discussion

In this study, we derived the first set of whole-brain voxel-wise heatmaps quantifying developmental changes of functional connectivity across the first six years of life. Globally, whole-brain functional connectivity changes featured a nonlinear pattern with 0−1 showing more changes than 1−2, but picking up speed by 2−4, which demonstrated more changes than 4−6 and other age spans. Males and females shared similar patterns at the voxel-level, but at the global level, females showed greater developmental changes during the first year of life and fewer changes during the second year while males did not, indicating that the overall global difference observed between 0−1 and 1−2 may be driven by girls. It is important to note the caveat of a brain state change between 2 and 4 years of age (i.e., from natural sleep to awake cartoon watching), which may have influenced the changes observed in this age span and should be carefully considered. Limbic and subcortical regions consistently showed the most developmental changes in their functional connectivity patterns across all four examined age spans, followed by changes in other higher-order regions, with primary sensory regions showing the least change over time. These patterns were consistent across full-term and preterm subgroups. Further validation on two randomly divided subsamples revealed global patterns consistent with the main findings. Importantly, these global and age-dependent patterns held in an independent cross-sectional sample, supporting the robustness of the observed developmental trends.

4.1. Developmental changes: global patterns

In line with previous work showing nonlinear developmental patterns (Gao et al., 2011, 2017; Grayson and Fair, 2017; Zhang et al., 2019), more developmental changes in functional connectivity were observed during the first (0−1) compared with the second postnatal year (1−2). During the first year of life, many networks undergo dynamic changes with the maturational sequence of functional connectivity paralleling the pattern of behavioral milestones across development (Keunen et al., 2017). We observed the greatest changes in limbic areas across the first year (0−1), consistent with the rapid development of functional connections involved in the default mode (Gao et al., 2009, 2017), salience, hippocampus, and amygdala networks, (Atzil et al., 2018; Gao et al., 2009, 2015a, 2015b; Salzwedel et al., 2019) during this time period. Interestingly, when we separated the original cohort into male and female subgroups, female infants showed more developmental

changes during the first year (i.e., 0−1) and fewer changes during the second year (i.e., 1−2) while males did not, suggesting that the global differences observed in the original combined cohort (i.e., more developmental changes observed during 0−1 compared with the 1−2) may have been driven by girls in the sample. This intriguing finding indicates that girls may experience earlier maturation of functional connectivity with more dynamic changes occurring during the first year than boys. If independently validated, such a pattern may have the potential to explain the observed differences in behavioral development between girls and boys at these early ages (e.g., more advanced verbal and non-verbal cognitive abilities in girls at this age; Galsworthy et al., 2000). In the later age spans (i.e., 2−4 and 4−6), males and females had comparable degrees of developmental changes. Taken together, these findings are in line with prior work indicating that sex-related effects may exhibit a unique developmental trajectory whereby sex differences are more prominent during certain developmental stages but negligible during others (Etchell et al., 2018). Although there has been substantial work examining sex differences in later childhood and adolescence (Kaczkurkin et al., 2019), little is known about sex differences during early neural development. Studies from other groups with independent cohorts are needed to validate the intriguing sex-dependent pattern observed in this study.

The most changes in functional connectivity were observed from 2−4 years of age (2−4). Although this was a bit surprising given the substantial body of work demonstrating the most dramatic structural brain development during the first two years (Gao et al., 2017; Gilmore et al., 2018), it is important to note that the developmental period from 2−4 years of age features equal, if not more, behavioral changes as the first two years of life (Kochanska et al., 2001; Richardson et al., 2018). Therefore, this finding is consistent with the dramatic development in various higher-order neurocognitive domains that begins to emerge from 2−4 years of age and continues to develop through age 6 and beyond (Korkman et al., 2001, 2013; Lebel et al., 2019; Richardson et al., 2018). Specifically, executive function and response inhibition have been shown to be supported by underlying functional connectivity development in associated networks during early to mid-childhood (Engelhardt et al., 2019; Fiske and Holmboe, 2019; Mehnert et al., 2013). As such, the functional connectivity changes we observed in 2−4 as well as 4−6 may reflect the corresponding development of functional connections that underlie these dramatic behavioral changes during this critical period. An important caveat to note in this study relates to a change in brain state across this age span (i.e., from natural sleep at age 2 to watching cartoons at age 4), which may account for part of the increase in the developmental changes observed. There was also an additional change in brain state during the 4−6 age span; whereas all 4-year-olds watched cartoons during the scan, the 6-year-olds were split between watching cartoons and a fixation cross. No voxel-wise differences were observed in a post-hoc comparison of two subgroups based on brain state between 4 and 6 (Cartoon-Cartoon and Cartoon-Cross), indicating that voxel-wise findings for this age span (4−6) were likely not influenced by differences in brain state changes. However, the Cartoon-Cartoon subgroup showed more whole-brain-level changes than the Cartoon-Cross subgroup, which may be due to the different cartoons the subjects watched at each time point. Indeed, prior work has demonstrated that even within the same setting of watching cartoons, different cartoon stimuli can induce different brain responses (i.e., different magnitudes of evoked responses to different events) in children as young as 3 years of age (Richardson et al., 2018). This is an important limitation of the current study; future work in populations with more homogenous brain states is needed to validate these findings, although we recognize the practical challenge of imaging 4-year-olds during natural sleep (or imaging 2-year-olds while awake). Taken together, with brain state-related differences in mind, dynamic changes observed in the two older age spans may reflect the development of higher-order regions and networks that continue to develop well into later childhood and adolescence (Casey et al., 2000; Larsen and Luna, 2018).

4.2. Developmental changes: network-level patterns

Different functional systems have been shown to exhibit distinct developmental trajectories with an overarching hierarchical developmental order proceeding from primary functional systems to higher-order networks (Gao et al., 2015a; 2015b; Zhang et al., 2019). Consistent with this, we observed the fewest changes (i.e., most stability) in primary sensory networks/regions including the visual and sensorimotor areas, followed by more developmental changes in higher-order networks including frontoparietal, ventral attention, dorsal attention, and default mode networks, with limbic and subcortical networks consistently demonstrating the most changes in functional connectivity across all four age spans. This was further supported by the consistent pattern we observed across all five age groups whereby primary networks (including visual and somatomotor networks) showed fewer intra- and inter-network developmental changes whereas higher-order networks (including subcortical, limbic and frontoparietal networks) demonstrated more intra- and inter-network developmental changes (Figure S9).

Primary visual and sensorimotor networks can already be detected *in utero* (Thomason et al., 2015); at birth, these networks show adult-like topology at birth in both premature infants at term age (Doria et al., 2010; Fransson et al., 2007, 2011; Smyser et al., 2010) as well as in full-term neonates (Gao et al., 2015a; 2015b), with minimal changes during the first year of life (Gao et al., 2015a; 2015b). The visual network in particular has consistently been found to develop the earliest (Gao et al., 2015a; 2015b). Indeed, visual processing provides an important foundation for the maturation of other higher-order functional networks that rely on visual information processing, including attention networks (Zhang et al., 2019). This may serve to enable the enriched development of higher-order association regions including attention and default mode networks across the first year of life (Cao et al., 2017; Gao et al., 2015a; 2015b). In line with this, primary visual and sensorimotor networks exhibited the fewest changes from neonate to 6 years of age. By contrast, higher-order networks including frontoparietal control, attention, and default mode networks demonstrated more changes over time, consistent with prior findings that executive functions undergo a protracted developmental period (Rothbart et al., 2011).

Across all four age spans we examined, limbic and subcortical networks consistently showed the greatest degree of functional reorganization as well as intra- and inter-network development across time. Prior work has demonstrated that subcortical regions undergo significant development during the first postnatal year (Alcauter et al., 2014; Toulmin et al., 2015). For example, although thalamocortical connectivity to primary sensory areas is relatively mature at birth, thalamocortical connectivity to other higher-order networks (e.g., salience and default mode networks) emerges towards the end of the first year of life through the second year (Alcauter et al., 2014). Limbic and subcortical regions also play a significant role in socioemotional development (Casey et al., 2019), which is critical for the successful establishment of effective social interaction routines and emotional regulation capabilities, which in turn are fundamental for learning as well as the emergence of other cognitive and executive functions (Atzil et al., 2018; Pessoa, 2008). Here we demonstrate that limbic and subcortical functional circuits underlying these behaviors undergo the most dramatic developmental changes from birth to 6 years of age, highlighting the importance of these structures across the entire early brain development period. Consistent with these findings, protracted experience-dependent development of socioemotional functions during early to mid-childhood is crucial for forming the basis of personality and socioemotional regulation (Atzil et al., 2018; Feldman, 2015; Herba, 2014; Raby et al., 2015). Therefore, the observed constant reorganization of the brain's arousal/social/emotional circuits during the first 6 years of life likely arises from the need to adapt to both the ever-changing external social environment as well as the ever-increasing internal capacity for engaging in social interactions, learning, and regulating. Thus, the

network-level developmental changes we observed may largely reflect the emergence and utilization of "transient" or "age-specific" strategies give internal functional limits to maximize the opportunity for learning and adaptation.

4.3. Robustness of the findings

Post hoc analyses examining the effect of term status, validation by splitting the original cohort randomly, and verification by comparing with an independent cross-sectional sample revealed patterns that were highly consistent with our main findings. Subtle differences between the main results from the original mixed-longitudinal cohort and the independent cross-sectional sample may be related to elevated inter-subject variability in the cross-sectional sample (Gao et al., 2014).

4.4. Limitations

Several limitations warrant further discussion. Neonates, 1-year-olds, and 2-year-olds were scanned during natural sleep, whereas 4-year-olds watched cartoons and 6-year-olds either watched cartoons or a fixation cross. Thus, the age span that included 2- and 4-year-olds (i. e., 2−4) included a change in brain state (i.e., natural sleep to watching cartoons) that we were unable to account for. Furthermore, the final age span (i.e., 4−6) also included an additional change in brain state (i.e., Cartoon-Cartoon: watching different cartoons at 4 and 6; Cartoon-Cross: cartoons at 4 and fixation cross at 6). Although no significant voxel-wise differences were found between the Cartoon-Cartoon subgroup versus the Cartoon-Cross subgroup, future studies with more homogenous brain states are needed to validate these findings. Relatedly, even though all neonates, 1-, and 2-year-olds were scanned during natural sleep, there could be potential sleep state differences across the first two years of life (Mitra et al., 2017), which may have also contributed to the observed developmental changes. However, the gold-standard of simultaneous EEG-fMRI recordings to determine sleep state faces great challenges in its practical application in scanning naturally sleeping infants. Future efforts are needed to address this. Lastly, another limitation is the relatively short rsfMRI scan (3 min). Although reliability may decrease with rsfMRI data shorter than 10 min (Gordon et al., 2017), previous work has shown that functional connectivity is reliable and stable for scans between 3 and 12 min in length (Braun et al., 2012; Van Dijk et al., 2010). In addition, we have previously used 3-minute rsfMRI data to robustly detect functional connectivity in this same population of infants and young children (Chen et al., 2021; J. Liu et al., 2021; Salzwedel et al., 2019). Furthermore, the large sample size used in this study, particularly in the first few time points, provides enough power for the reliable detection of functional connectivity (Zuo et al., 2019). Although the sample sizes for the brain state change subgroups were relatively small (Cartoon-Cartoon: N = 28; Cartoon-Cross: N = 22), prior work has demonstrated acceptable reliability for group analyses with at least 20 subjects (Thirion et al., 2007). However, future large-scale studies with longer individual fMRI data are needed to fully address this limitation.

5. Conclusions

To our knowledge, this is the first study to set forth a series of whole-brain heatmaps quantifying voxel-level developmental changes in functional connectivity across the first six years of life. Our findings highlight a globally nonlinear pattern featuring more changes during the first year than the second, followed by another period of highly dramatic changes from 2 to 6 years of age. Intriguingly, sex differences were observed suggesting that the nonlinear developmental patterns during the first two years may have been driven by females. Independent validation is needed for this finding. Regionally, limbic and subcortical regions consistently showed the most dynamic changes whereas primary areas remained stable across the first 6 years of life, shedding insight on

the critical regions/periods of early brain development. Overall, the set of whole-brain developmental heatmaps derived in this study contribute to a better understanding of the dynamics underlying early brain functional development.

Data statement

Infant participants were part of the University of North Carolina Early Brain Development Study. Informed consent was obtained from parents/legal guardians of infant participants under protocols approved by the University of North Carolina at Chapel Hill and Cedars-Sinai Institutional Review Board (IRB). After quality control, a cohort of 655 subjects (full-term: N = 364, preterm: N = 291) with successful rsfMRI scans for at least one time point were retrospectively identified and included in this study. Time points included 3 weeks (neonate), 1 year, 2 year, 4 year, and 6 year. Among them, 266 subjects (full-term: N = 140, preterm: N = 126) had successful rsfMRI scans on at least two consecutive time points. Consecutive time points included 3 weeks and 1 year (0−1), 1 year and 2 year (1−2), 2 year and 4 year (2−4), as well as 4 year and 6 year (4−6). Criteria for determining full-term and preterm required gestational age at birth > = 37 weeks or <37 weeks, respectively. Exclusionary criteria included any neonatal illness requiring more than a 24 -h stay at a neonatal intensive care unit, abnormal MRI, major medical/neurologic illness, psychiatric problems, and maternal psychiatric disorder diagnosis.

Appendix A. Supplementary data

Supplementary material related to this article can be found, in the online version, at doi:https://doi.org/10.1016/j.dcn.2021.100976.

References

Alcauter, S., Lin, W., Keith Smith, J., Short, S.J., Goldman, B.D., Steven Reznick, J., Gilmore, J.H., Gao, W., 2014. Development of thalamocortical connectivity during infancy and its cognitive correlations. J. Neurosci. 34 (27), 9067–9075. https://doi.org/10.1523/JNEUROSCI.0796-14.2014.

Andersson, J.L.R., Jenkinson, M., Smith, S., 2007. Non-linear Registration Aka Spatial Normalisation FMRIB Technial Report TR07JA2.

Atzil, S., Gao, W., Fradkin, I., Barrett, L.F., 2018. Growing a social brain. Nat. Hum. Behav. 2 (9), 624–636. https://doi.org/10.1038/s41562-018-0384-6. Nature Publishing Group.

Benjamini, Y., Hochberg, Y., 1995. Controlling the false discovery rate: a practical and powerful approach to multiple testing. J. R. Stat. Soc. Ser. B 57 (1), 289–300. https://doi.org/10.1111/j.2517-6161.1995.tb02031.x.

Braun, U., Plichta, M.M., Esslinger, C., Sauer, C., Haddad, L., Grimm, O., Mier, D., Mohnke, S., Heinz, A., Erk, S., Walter, H., Seiferth, N., Kirsch, P., Meyer-Lindenberg, A., 2012. Test-retest reliability of resting-state connectivity network

characteristics using fMRI and graph theoretical measures. NeuroImage 59 (2), 1404–1412. https://doi.org/10.1016/j.neuroimage.2011.08.044.

Brenner, R.G., Smyser, C.D., Lean, R.E., Kenley, J.K., Smyser, T.A., Cyr, P.E.P., Shimony, J.S., Barch, D.M., Rogers, C.E., 2020. Microstructure of the dorsal anterior cingulum bundle in very preterm neonates predicts the preterm behavioral phenotype at 5 years of age. Biol. Psychiatry. https://doi.org/10.1016/j.biopsych.2020.06.015.

Cao, M., He, Y., Dai, Z., Liao, X., Jeon, T., Ouyang, M., Chalak, L., Bi, Y., Rollins, N., Dong, Q., Huang, H., 2017. Early development of functional network segregation revealed by connectomic analysis of the preterm human brain. Cereb. Cortex 27 (3), 1949–1963. https://doi.org/10.1093/cercor/bhw038.

Casey, B.J., Giedd, J.N., Thomas, K.M., 2000. Structural and functional brain development and its relation to cognitive development. Biol. Psychol. 54 (1–3), 241–257. https://doi.org/10.1016/S0301-0511(00)00058-2.

Casey, B.J., Heller, A.S., Gee, D.G., Cohen, A.O., 2019. Development of the emotional brain. Neurosci. Lett. 693, 29–34. https://doi.org/10.1016/j.neulet.2017.11.055. Elsevier Ireland Ltd.

Chen, Y., Liu, S., Salzwedel, A., Stephens, R., Cornea, E., Goldman, B.D., Gilmore, J.H., Gao, W., 2021. The subgrouping structure of newborns with heterogenous brain–Behavior relationships. Cereb. Cortex 31 (1), 301–311. https://doi.org/10.1093/cercor/bhaa226.

Conboy, B.T., Sommerville, J.A., Kuhl, P.K., 2008. Cognitive control factors in speech perception at 11 months. Dev. Psychol. 44 (5), 1505–1512. https://doi.org/10.1037/a0012975.

Cox, R.W., 1996. AFNI: software for analysis and visualization of functional magnetic resonance neuroimages. Comput. Biomed. Res. 29 (3), 162–173. https://doi.org/10.1006/cbmr.1996.0014.

Cserjesi, R., Van Braeckel, K.N.J.A., Timmerman, M., Butcher, P.R., Kerstjens, J.M., Reijneveld, S.A., Bouma, A., Bos, A.F., Geuze, R.H., 2012. Patterns of functioning and predictive factors in children born moderately preterm or at term. Dev. Med. Child Neurol. 54 (8), 710–715. https://doi.org/10.1111/j.1469-8749.2012.04328.x.

Doria, V., Beckmann, C.F., Arichi, T., Merchant, N., Groppo, M., Turkheimer, F.E., Counsell, S.J., Murgasova, M., Aljabar, P., Nunes, R.G., Larkman, D.J., Rees, G., Edwards, A.D., 2010. Emergence of resting state networks in the preterm human brain. Proc. Natl. Acad. Sci. U.S.A. 107 (46), 20015–20020. https://doi.org/10.1073/pnas.1007921107.

Engelhardt, L.E., Harden, K.P., Tucker-Drob, E.M., Church, J.A., 2019. The neural architecture of executive functions is established by middle childhood. NeuroImage 185, 479–489. https://doi.org/10.1016/j.neuroimage.2018.10.024.

Etchell, A., Adhikari, A., Weinberg, L.S., Choo, A.L., Garnett, E.O., Chow, H.M., Chang, S. E., 2018. A systematic literature review of sex differences in childhood language and brain development. Neuropsychologia 114, 19–31. https://doi.org/10.1016/j.neuropsychologia.2018.04.011. Elsevier Ltd.

Feldman, R., 2015. The adaptive human parental brain: implications for children's social development. Trends Neurosci. 38 (6), 387–399. https://doi.org/10.1016/j.tins.2015.04.004. Elsevier Ltd.

Fiske, A., Holmboe, K., 2019. Neural substrates of early executive function development. Dev. Rev. 52, 42–62. https://doi.org/10.1016/j.dr.2019.100866. Mosby Inc.

Fransson, P., Skiöld, B., Horsch, S., Nordell, A., Blennow, M., Lagercrantz, H., Åden, U., 2007. Resting-state networks in the infant brain. Proc. Natl. Acad. Sci. U.S.A. 104 (39), 15531–15536. https://doi.org/10.1073/pnas.0704380104.

Fransson, P., Den, U.A., Lagercrantz, H., 2011. The functional architecture of the infant brain as revealed by resting-state fMRI. Cereb. Cortex 21, 145–154. https://doi.org/10.1093/cercor/bhq071.

Galsworthy, M.J., Dionne, G., Dale, P.S., Plomin, R., 2000. Sex differences in early verbal and non-verbal cognitive development. Dev. Sci. 3 (2), 206–215. https://doi.org/10.1111/1467-7687.00114.

Gao, W., Zhu, H., Giovanello, K.S., Smith, J.K., Shen, D., Gilmore, J.H., Lin, W., 2009. Evidence on the emergence of the brain's default network from 2-week-old to 2-year-old healthy pediatric subjects. Proc. Natl. Acad. Sci. U.S.A. 106 (16), 6790–6795. https://doi.org/10.1073/pnas.0811221106.

Gao, W., Gilmore, J.H., Giovanello, K.S., Smith, J.K., Shen, D., Zhu, H., Lin, W., 2011. Temporal and spatial evolution of brain network topology during the first two years of life. PLoS One 6 (9), e25278. https://doi.org/10.1371/journal.pone.0025278.

Gao, W., Elton, A., Zhu, H., Alcauter, S., Smith, J.K., Gilmore, J.H., Lin, W., 2014. Intersubject variability of and genetic effects on the Brain's functional connectivity during infancy. J. Neurosci. 34 (34), 11288–11296. https://doi.org/10.1523/JNEUROSCI.5072-13.2014.

Gao, W., Alcauter, S., Elton, A., Hernandez-Castillo, C.R., Smith, J.K., Ramirez, J., Lin, W., 2015a. Functional network development during the first year: relative sequence and socioeconomic correlations. Cereb. Cortex 25 (9), 2919–2928. https://doi.org/10.1093/cercor/bhu088.

Gao, W., Alcauter, S., Smith, J.K., Gilmore, J.H., Lin, W., 2015b. Development of human brain cortical network architecture during infancy. Brain Struct. Funct. 220 (2), 1173–1186. https://doi.org/10.1007/s00429-014-0710-3.

Gao, W., Lin, W., Grewen, K., Gilmore, J.H., 2017. Functional connectivity of the infant human brain: plastic and modifiable. Neuroscientist 23 (2), 169–184. https://doi.org/10.1177/1073858416635986. SAGE Publications Inc.

Gao, W., Grewen, K., Knickmeyer, R.C., Qiu, A., Salzwedel, A., Lin, W., Gilmore, J.H., 2019. A review on neuroimaging studies of genetic and environmental influences on early brain development. NeuroImage 185, 802–812. https://doi.org/10.1016/j.neuroimage.2018.04.032. Academic Press Inc.

Gao, W., Chen, Y., Cornea, E., Goldman, B.D., Gilmore, J.H., 2020. Neonatal brain connectivity outliers identify over forty percent of IQ outliers at 4 years of age. Brain Behav. 10 (12), e01846. https://doi.org/10.1002/brb3.1846.

Gilmore, J.H., Knickmeyer, R.C., Gao, W., 2018. Imaging structural and functional brain development in early childhood. Nat. Rev. Neurosci. 19 (3), 123–137. https://doi.org/10.1038/nrn.2018.1. Nature Publishing Group.

Gordon, E.M., Laumann, T.O., Gilmore, A.W., Newbold, D.J., Greene, D.J., Berg, J.J., Ortega, M., Hoyt-Drazen, C., Gratton, C., Sun, H., Hampton, J.M., Coalson, R.S., Nguyen, A.L., McDermott, K.B., Shimony, J.S., Snyder, A.Z., Schlaggar, B.L., Petersen, S.E., Nelson, S.M., Dosenbach, N.U.F., 2017. Precision functional mapping of individual human brains. Neuron 95 (4), 791–807. https://doi.org/10.1016/j.neuron.2017.07.011 e7.

Grayson, D.S., Fair, D.A., 2017. Development of large-scale functional networks from birth to adulthood: a guide to the neuroimaging literature. NeuroImage 160, 15–31. https://doi.org/10.1016/j.neuroimage.2017.01.079.

Herba, C.M., 2014. Maternal depression and child behavioural outcomes. Lancet Psychiatry 1 (6), 408–409. https://doi.org/10.1016/S2215-0366(14)70375-X. Elsevier Ltd.

Hyvärinen, A., Oja, E., 2000. Independent component analysis: algorithms and applications. Neural Netw. 13 (4–5), 411–430. https://doi.org/10.1016/S0893-6080(00)00026-5.

Jenkinson, M., Bannister, P., Brady, M., Smith, S., 2002. Improved optimization for the robust and accurate linear registration and motion correction of brain images. NeuroImage 17 (2), 825–841. https://doi.org/10.1006/nimg.2002.1132.

Jiang, Z.D., Wilkinson, A.R., 2008. Normal brainstem responses in moderately preterm infants. Acta Paediatr. 97 (10), 1366–1369. https://doi.org/10.1111/j.1651-2227.2008.00935.x.

Joshi, A.A., Chong, M., Li, J., Choi, S., Leahy, R.M., 2018. Are you thinking what I'm thinking? Synchronization of resting fMRI time-series across subjects. NeuroImage 172, 740–752. https://doi.org/10.1016/j.neuroimage.2018.01.058.

Kaczkurkin, A.N., Raznahan, A., Satterthwaite, T.D., 2019. Sex differences in the developing brain: insights from multimodal neuroimaging. Neuropsychopharmacology 44 (1), 71–85. https://doi.org/10.1038/s41386-018-0111-z. Nature Publishing Group.

Keunen, K., Counsell, S.J., Benders, M.J.N.L., 2017. The emergence of functional architecture during early brain development. NeuroImage 160, 2–14. https://doi.org/10.1016/j.neuroimage.2017.01.047.

Kochanska, G., Coy, K.C., Murray, K.T., 2001. The development of self-regulation in the first four years of life. Child Dev. 72 (4), 1091–1111. https://doi.org/10.1111/1467-8624.00336.

Korkman, M., Kemp, S.L., Kirk, U., 2001. Effects of age on neurocognitive measures of children ages 5 to 12: A cross-sectional study on 800 children from the United States. Dev. Neuropsychol. 20 (1), 331–354. https://doi.org/10.1207/S15326942DN2001_2.

Korkman, M., Lahti-Nuuttila, P., Laasonen, M., Kemp, S.L., Holdnack, J., 2013. Neurocognitive development in 5-to 16-year-old North American children: a cross-sectional study. Child Neuropsychol. 19 (5), 516–539. https://doi.org/10.1080/09297049.2012.705822.

Larsen, B., Luna, B., 2018. Adolescence as a neurobiological critical period for the development of higher-order cognition. Neurosci. Biobehav. Rev. 94, 179–195. https://doi.org/10.1016/j.neubiorev.2018.09.005. Elsevier Ltd.

Lebel, C., Treit, S., Beaulieu, C., 2019. A review of diffusion MRI of typical white matter development from early childhood to young adulthood. NMR Biomed. 32 (4), e3778. https://doi.org/10.1002/nbm.3778.

Lee, M.H., Smyser, C.D., Shimony, J.S., 2013. Resting-state fMRI: a review of methods and clinical applications. Am. J. Neuroradiol. 34 (10), 1866–1872. https://doi.org/10.3174/ajnr.A3263.

Liu, Z., Ke, L., Liu, H., Huang, W., Hu, Z., 2014. Changes in topological organization of functional PET brain network with normal aging. PLoS One 9 (2), 88690. https://doi.org/10.1371/journal.pone.0088690.

Liu, J., Chen, Y., Stephens, R., Cornea, E., Goldman, B., Gilmore, J.H., Gao, W., 2021. Hippocampal Functional Connectivity Development during the First Two Years Indexes 4-year Working Memory Performance. Cortex. https://doi.org/10.1016/j.cortex.2021.02.005.

Manning, J.H., Courchesne, E., Fox, P.T., 2013. Intrinsic connectivity network mapping in young children during natural sleep. NeuroImage 83, 288–293. https://doi.org/10.1016/j.neuroimage.2013.05.020.

Mehnert, J., Akhrif, A., Telkemeyer, S., Rossi, S., Schmitz, C.H., Steinbrink, J., Wartenburger, I., Obrig, H., Neufang, S., 2013. Developmental changes in brain activation and functional connectivity during response inhibition in the early childhood brain. Brain Dev. 35 (10), 894–904. https://doi.org/10.1016/j.braindev.2012.11.006.

Mitra, A., Snyder, A.Z., Tagliazucchi, E., Laufs, H., Elison, J., Emerson, R.W., Shen, M.D., Wolff, J.J., Botteron, K.N., Dager, S., Estes, A.M., Evans, A., Gerig, G., Hazlett, H.C., Paterson, S.J., Schultz, R.T., Styner, M.A., Zwaigenbaum, L., Schlaggar, B.L., Raichle, M., 2017. Resting-state fMRI in sleeping infants more closely resembles adult sleep than adult wakefulness. PLoS One 12 (11), e0188122. https://doi.org/10.1371/journal.pone.0188122.

Monk, C., Lugo-Candelas, C., Trumpff, C., 2019. Prenatal developmental origins of future psychopathology: mechanisms and pathways. Annu. Rev. Clin. Psychol. 15 (1), 317–344. https://doi.org/10.1146/annurev-clinpsy-050718-095539.

Pessoa, L., 2008. On the relationship between emotion and cognition. Nat. Rev. Neurosci. 9 (2), 148–158. https://doi.org/10.1038/nrn2317. Nature Publishing Group.

Power, J.D., Cohen, A.L., Nelson, S.M., Wig, G.S., Barnes, K.A., Church, J.A., Vogel, A.C., Laumann, T.O., Miezin, F.M., Schlaggar, B.L., Petersen, S.E., 2011. Functional network organization of the human brain. Neuron 72 (4), 665–678. https://doi.org/10.1016/j.neuron.2011.09.006.

Power, J.D., Barnes, K.A., Snyder, A.Z., Schlaggar, B.L., Petersen, S.E., 2012. Spurious but systematic correlations in functional connectivity MRI networks arise from

subject motion. NeuroImage 59 (3), 2142–2154. https://doi.org/10.1016/j.neuroimage.2011.10.018.

Power, J.D., Mitra, A., Laumann, T.O., Snyder, A.Z., Schlaggar, B.L., Petersen, S.E., 2014. Methods to detect, characterize, and remove motion artifact in resting state fMRI. NeuroImage 84, 320–341. https://doi.org/10.1016/j.neuroimage.2013.08.048.

Raby, K.L., Roisman, G.I., Simpson, J.A., Collins, W.A., Steele, R.D., 2015. Greater maternal insensitivity in childhood predicts greater electrodermal reactivity during conflict discussions with romantic partners in adulthood. Psychol. Sci. 26 (3), 348–353. https://doi.org/10.1177/0956797614563340.

Richardson, H., Lisandrelli, G., Riobueno-Naylor, A., Saxe, R., 2018. Development of the social brain from age three to twelve years. Nat. Commun. 9 (1), 1–12. https://doi.org/10.1038/s41467-018-03399-2.

Rothbart, M.K., Sheese, B.E., Rueda, M.R., Posner, M.I., 2011. Developing mechanisms of self-regulation in early life. Emotion Rev.: J. Int. Soc. Res. Emotion 3 (2), 207–213. https://doi.org/10.1177/1754073910387943.

Salzwedel, A.P., Stephens, R.L., Goldman, B.D., Lin, W., Gilmore, J.H., Gao, W., 2019. Development of amygdala functional connectivity during infancy and its relationship with 4-Year behavioral outcomes. Biol. Psychiatry Cogn. Neurosci. Neuroimaging 4 (1), 62–71. https://doi.org/10.1016/j.bpsc.2018.08.010.

Shi, F., Yap, P.-T., Wu, G., Jia, H., Gilmore, J.H., Lin, W., Shen, D., 2011. Infant Brain Atlases from Neonates to 1- and 2-Year-Olds. PLoS One 6 (4), e18746. https://doi.org/10.1371/journal.pone.0018746.

Smith, S.M., Jenkinson, M., Woolrich, M.W., Beckmann, C.F., Behrens, T.E.J., Johansen-Berg, H., Bannister, P.R., De Luca, M., Drobnjak, I., Flitney, D.E., Niazy, R.K., Saunders, J., Vickers, J., Zhang, Y., De Stefano, N., Brady, J.M., Matthews, P.M., 2004. Advances in functional and structural MR image analysis and implementation as FSL. NeuroImage 23 (SUPPL. 1). https://doi.org/10.1016/j.neuroimage.2004.07.051.

Smyser, C.D., Inder, T.E., Shimony, J.S., Hill, J.E., Degnan, A.J., Snyder, A.Z., Neil, J.J., 2010. Longitudinal analysis of neural network development in preterm infants. Cereb. Cortex 20, 2852–2862. https://doi.org/10.1093/cercor/bhq035.

Thirion, B., Pinel, P., Mériaux, S., Roche, A., Dehaene, S., Poline, J.B., 2007. Analysis of a large fMRI cohort: statistical and methodological issues for group analyses. NeuroImage 35 (1), 105–120. https://doi.org/10.1016/j.neuroimage.2006.11.054.

Thomason, M.E., Grove, L.E., Lozon, T.A., Vila, A.M., Ye, Y., Nye, M.J., Manning, J.H., Pappas, A., Hernandez-Andrade, E., Yeo, L., Mody, S., Berman, S., Hassan, S.S., Romero, R., 2015. Age-related increases in long-range connectivity in fetal functional neural connectivity networks in utero. Dev. Cogn. Neurosci. 11, 96–104. https://doi.org/10.1016/j.dcn.2014.09.001.

Toulmin, H., Beckmann, C.F., O'Muircheartaigh, J., Ball, G., Nongena, P., Makropoulos, A., Ederies, A., Counsell, S.J., Kennea, N., Arichi, T., Tusor, N., Rutherford, M.A., Azzopardi, D., Gonzalez-Cinca, N., Hajnal, J.V., Edwards, A.D., 2015. Specialization and integration of functional thalamocortical connectivity in the human infant. Proc. Natl. Acad. Sci. U.S.A. 112 (20), 6485–6490. https://doi.org/10.1073/pnas.1422638112.

Van Dijk, K.R.A., Hedden, T., Venkataraman, A., Evans, K.C., Lazar, S.W., Buckner, R.L., 2010. Intrinsic functional connectivity as a tool for human connectomics: theory, properties, and optimization. J. Neurophysiol. 103 (1), 297–321. https://doi.org/10.1152/jn.00783.2009.

Volkow, N.D., Gordon, J.A., Freund, M.P., 2020. The healthy brain and child development study-shedding light on opioid exposure, COVID-19, and health disparities. JAMA Psychiatry. American Medical Association. https://doi.org/10.1001/jamapsychiatry.2020.3803.

Wadhwa, P.D., Buss, C., Entringer, S., Swanson, J.M., 2009. Developmental origins of health and disease: brief history of the approach and current focus on epigenetic mechanisms. Semin. Reprod. Med. 27 (5), 358–368. https://doi.org/10.1055/s-0029-1237424. NIH Public Access.

Yeo, B.T.T., Krienen, F.M., Sepulcre, J., Sabuncu, M.R., Lashkari, D., Hollinshead, M., Roffman, J.L., Smoller, J.W., Zöllei, L., Polimeni, J.R., Fisch, B., Liu, H., Buckner, R.L., 2011. The organization of the human cerebral cortex estimated by intrinsic functional connectivity. J. Neurophysiol. 106 (3), 1125–1165. https://doi.org/10.1152/jn.00338.2011.

Zhang, H., Shen, D., Lin, W., 2019. Resting-state functional MRI studies on infant brains: a decade of gap-filling efforts. NeuroImage 185, 664–684. https://doi.org/10.1016/j.neuroimage.2018.07.004. Academic Press Inc.

Zuo, X.N., Xu, T., Milham, M.P., 2019. Harnessing reliability for neuroscience research. Nat. Hum. Behav. 3 (8), 768–771. https://doi.org/10.1038/s41562-019-0655-x. Nature Research.